No. O-017

A Study on Influence of Induction Motor Model on Power System Stability

DAHAL, Sudarshan ATTAVIRIYANUPAP, Pathom and KATAOKA, Yoshihiko
Tokyo Institute of Technology
2-12-1 Ookayama, Meguro-ku, Tokyo 152-8550, Japan

Abstract

This paper presents the comparative study of influence of induction motor models in power system stability studies. The fifth order, third order and the first order induction motor models have been developed in the rotor reference frame. This implementation eliminates the possible discontinuity of state variables due to step change in the phasor of the system. The simulation result shows that the responses of the three models are different under the same disturbance conditions. The system stability limit is constrained by the system loading level and applied ratio of induction motor. The transient/steady-state stability analysis shows that the first order model gives the most optimistic stability result.

Keywords: Induction motor model, power system stability, stability limit, eigenvalues

1 INTRODUCTION

The catastrophic consequences of blackouts in North America, Europe and even East Asian countries have urged the necessity of proper security assessment and planning for the stable operation of power system grids [1, 2, 3]. The accurate security assessment needs the accurate modeling of power system components. This is a great challenge for power engineers as the networks are becoming more and more complex and components show highly non-linear behavior [1,4]. Moreover, the load modeling has become difficult due to the random behavior of the load and the accumulation of large volume of data from the field measurement [4].

Modeling of the load has two major issues: modeling and parameter identification [4,5,6]. The field measurement data is used for the parameter identification of the composite load of the load bus [4]. The dynamic part of the composite loads is represented by induction motor in [1,4,5,6]. The power system stability is affected by the amount of the dynamic motor loads connected to the system and the line loading level. Correspondingly, the load behaviors are different for different system conditions [6]. So, choice of appropriate load model is important for the accuracy of system stability analysis.

Different models of induction motors are available in different literatures. In some power system stability studies[2,4,10], the third order model is employed for the simulations while the first order model is employed in some voltage stability studies. These different models use different levels of approximations possibly resulting in the insufficient modeling of the behavior of induction motor [7]. This, in turn, affects the accuracy of the stability analysis. In [8,9], comparative assessment of the accuracy of the different models is shown. However, comparative study from the viewpoint of power system stability has not been done sufficiently yet.

Induction motors are generally modeled in the frame synchronously rotating with system frequency [1-12]. However, disturbance in the system sometimes causes the step change in phase angle. This results in the discontinuity of the state variables of induction motors, i.e. the stator and rotor fluxes.

In this paper, first, we develop induction motor models of first order, third order and fifth order in a reference frame attached to rotor axis. We will implement these motors in a nine-bus power system. Assuming the response of the fifth order model as a most accurate one, we will compare the response of all the models under same set of disturbances. Second, we will evaluate the stability limit of the system implementing the different models of motor with different percentage of motor loads. Finally, we will perform the eigenvalue analysis of the system to compare the steady state stability of the system implementing different models of induction motor.

2 ANALYSIS OF INDUCTION MOTOR MODELS

2.1 Fifth, third and first order model in ω_e frame

The dynamics of induction motor can be represented by the set of five differential equations as shown in (1)[11].

$$
\begin{aligned}
v_{qs}^{e} &= \frac{p}{\omega_b}\psi_{qs}^{e} + \frac{\omega_e}{\omega_b}\psi_{ds}^{e} + r_s i_{qs}^{e} \\
v_{ds}^{e} &= \frac{p}{\omega_b}\psi_{ds}^{e} - \frac{\omega_e}{\omega_b}\psi_{qs}^{e} + r_s i_{ds}^{e} \\
v_{qr}^{'e} &= \frac{p}{\omega_b}\psi_{qr}^{'e} + \left(\frac{\omega_e - \omega_r}{\omega_b}\right)\psi_{dr}^{'e} + r_r^{'} i_{qr}^{'e} \\
v_{dr}^{'e} &= \frac{p}{\omega_b}\psi_{dr}^{'e} - \left(\frac{\omega_e - \omega_r}{\omega_b}\right)\psi_{qr}^{'e} + r_r^{'} i_{dr}^{'e} \\
2H\, p\left(\frac{\omega_r}{\omega_b}\right) &= T_{em} - T_{mech} \\
where,\ p &= \frac{d}{dt} : differential\ operator
\end{aligned} \tag{1}
$$

Here, v_{qs}^{e}, v_{ds}^{e}, $v_{qr}^{'e}, v_{dr}^{'e}$ represent the stator and rotor voltages, $\psi_{qs}^{e}, \psi_{ds}^{e}, \psi_{qr}^{'e}, \psi_{dr}^{'e}$ represent the stator and rotor fluxes, r_s, r_r are stator and rotor resistances, $i_{qs}^{e}, i_{ds}^{e}, i_{qr}^{'e}, i_{dr}^{'e}$ are stator and rotor currents, H is inertia constant and $\omega_r, \omega_b, \omega_e$ are the rotor speed, base frequency and supply frequency respectively. T_{em} is the electromagnetic torque and T_{mech} is the mechanical torque on the motor shaft. The implementation of this fifth-order model in stability study is not common because of the requirement for balancing of the degree of approximation with synchronous machines. However, this paper includes the fifth-order model implementation for comparison of the lower order models.

The third order model can be obtained by neglecting the dynamics of the stator fluxes and the first order can be obtained by neglecting the dynamics of both the stator and rotor fluxes. It can be easily shown that this first order model is equivalent to the well-known model expressed by phasor quantities [12].

The flux equation is given as

$$
\begin{bmatrix} \psi_{qs}^{e} \\ \psi_{ds}^{e} \\ \psi_{qr}^{'e} \\ \psi_{dr}^{'e} \end{bmatrix} = \begin{bmatrix} x_{ls}+x_m & 0 & x_m & 0 \\ 0 & x_{ls}+x_m & 0 & x_m \\ x_m & 0 & x_{lr}^{'}+x_m & 0 \\ 0 & x_m & 0 & x_{lr}^{'}+x_m \end{bmatrix} \begin{bmatrix} i_{qs}^{e} \\ i_{ds}^{e} \\ i_{qr}^{'e} \\ i_{dr}^{'e} \end{bmatrix} \tag{2}
$$

Here, x_{ls}, $x_{lr}^{'}$ and x_m are stator, rotor and mutual reactance respectively.

2.2 Discontinuity problem in ω_e frame models

In transient/steady-state stability simulation framework, voltages and currents are shown by phasors for the purpose of reducing computational requirement. This phasor-based computation framework allows time step of 10 [ms] while instantaneous value-based computation requires time step less than 1 [ms].

In phasor-based framework, both slow and step changes in phasors are permitted. This means phasors can change discontinuously and then results in unbounded frequency at the moment of discontinuity. This may result in discontinuous change in induction motor state variables or fluxes as shown in Appendix I. The authors consider that this is not a proper situation and is to be avoided if possible.

2.3 New ω_r frame models

2.3.1 Derivation

In the ω_r frame model, the d and q axes are rotating with the axis of ω_r or rotor speed just like synchronous machine model. We can write the induction motor equations in ω_r frame, by transforming the equations in ω_e frame by suitable angle. The transformation angle is the difference between the angles of ω_e and ω_r axis. The angle between their axes is changing with time. Let the instantaneous transformation angle be $(\delta_e - \delta_r)$. This is related to the frequency as

$$
\frac{d}{dt}\left(\delta_e - \delta_r\right) = \frac{d\delta_e}{dt} - \frac{d\delta_r}{dt} = \omega_e - \omega_r \tag{3}
$$

Note that ω_e and ω_r are variable. Using this transformation angle, we can make the transformation matrix to transform the induction motor equations from ω_e frame into ω_r frame. So,

$$
T(\delta_e - \delta_r) = \begin{bmatrix} \cos(\delta_e - \delta_r) & -\sin(\delta_e - \delta_r) \\ \sin(\delta_e - \delta_r) & \cos(\delta_e - \delta_r) \end{bmatrix} \tag{4}
$$

This suggests that we need one more integrator to obtain δ_r.

Now, the transformation from ω_e frame to ω_r frame can be performed as,

$$
\begin{bmatrix} v_{qs}^{r} \\ v_{ds}^{r} \end{bmatrix} = T\left(\delta_e - \delta_r\right) \begin{bmatrix} v_{qs}^{e} \\ v_{ds}^{e} \end{bmatrix} \tag{5}
$$

So our new induction motor equations in ω_r frame can be written as

$$
\begin{aligned}
v_{qs}^{r} &= \frac{p}{\omega_b}\psi_{qs}^{r} + \frac{\omega_r}{\omega_b}\psi_{ds}^{r} + r_s i_{qs}^{r} \\
v_{ds}^{r} &= \frac{p}{\omega_b}\psi_{ds}^{r} - \frac{\omega_r}{\omega_b}\psi_{qs}^{r} + r_s i_{ds}^{r} \\
v_{qr}^{'r} &= \frac{p}{\omega_b}\psi_{qr}^{'r} + r_r^{'} i_{qr}^{'r} \\
v_{dr}^{'r} &= \frac{p}{\omega_b}\psi_{dr}^{'r} + r_r^{'} i_{dr}^{'r}
\end{aligned} \tag{6}
$$

The equation of motion of the rotor and the flux equations are same as that of ω_e frame model. The rotor angle for the coordinate transformation can be obtained as

$$p\delta_r = \left(1 - \frac{\omega_r}{\omega_b}\right) \tag{7}$$

where the definitions of the symbols are same as those of ω_e frame model.

The lower order models can also be derived by neglecting the dynamics of the stator and rotor fluxes. The flux equation is similar to that of ω_e frame as in (2), but the quantities would be in ω_r frame.

2.3.2 Discussion on computational requirement

While the steady state quantities are constant in ω_e frame, those are sinusoidal in ω_r frame as shown in Figure 2.3.1. Although the quantities are sinusoidal in ω_r frame, the computational requirement is not high because, in general, the slip frequency is below 1 [Hz]. The time step of 10 [ms], which is commonly used in stability simulations, can be used without loss of accuracy.

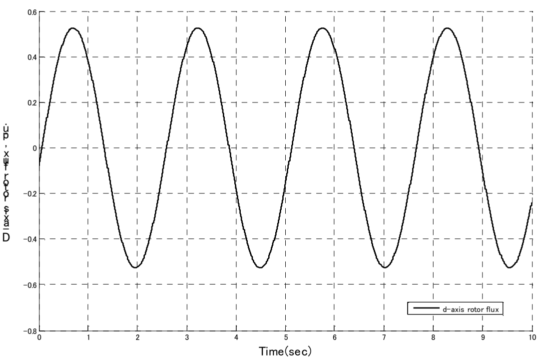

Figure 2.3.1 State variable (d-axis rotor flux) in ω_r frame

2.3.3 Evaluation of accuracy of ω_r frame model

The responses of the ω_r frame and ω_e frame models are compared. Since the first order model is expressed in terms of phasor quantities, both frames give the same equations. The third order model is widely used for stability analysis. So, the comparison of third order ω_r and ω_e frame models is presented. Neglecting the stator flux dynamics, the third order model in ω_r frame can be written as

$$v_{qs} = j\left(\frac{\omega_e - \omega_r}{\omega_b}\right)\psi_{qs} + \frac{\omega_r}{\omega_b}\psi_{ds} + r_s i_{qs}$$

$$v_{ds} = j\left(\frac{\omega_e - \omega_r}{\omega_b}\right)\psi_{ds} - \frac{\omega_r}{\omega_b}\psi_{qs} + r_s i_{ds}$$

$$0 = \frac{p}{\omega_b}\psi_{qr} + r_r i_{qr}$$

$$0 = \frac{p}{\omega_b}\psi_{dr} + r_r i_{dr} \tag{8}$$

Here, the subscripts have been removed for the simplicity of description. The equation of motion is same as (1). The flux linkage equations are similar to (2).

Simplification yields

$$v_{ds} + jv_{qs} = \left(r_s + \frac{j\omega_e}{\omega_b}\left(x_{ls} + x_m\right)\right)\left(i_{ds} + ji_{qs}\right) + \frac{j\omega_e}{\omega_b}x_m\left(i_{dr} + ji_{qr}\right)$$

Neglecting the frequency dependence of the impedance parameters we get the equivalent equation of induction motor in ω_r frame.

$$v_{ds} + jv_{qs} = \left(R_s + jX_s'\right)\left(i_{ds} + ji_{qs}\right) + \left(e_d + je_q\right) \tag{9}$$

where

$$R_s = r_s \qquad X_s' = \left((x_{ls} + x_m) - \frac{x_m^2}{\left(x_{lr} + x_m\right)}\right)$$

$$e_d = -\frac{x_m}{\left(x_{lr} + x_m\right)}\psi_{qr} \qquad e_q = \frac{x_m}{\left(x_{lr} + x_m\right)}\psi_{dr}$$

Third order dynamic equations of induction motor can be written as,

$$\frac{p}{\omega_b}e_d = -\frac{1}{T_o'}\left[e_d + \frac{x_m^2}{\left(x_{lr} + x_m\right)}i_{qs}\right]$$

$$\frac{p}{\omega_b}e_q = -\frac{1}{T_o'}\left[e_q - \frac{x_m^2}{\left(x_{lr} + x_m\right)}i_{ds}\right]$$

$$2H\frac{d}{dt}\left(\frac{\omega_r}{\omega_b}\right) = T_{em} - T_{mech} \tag{10}$$

where $T_o' = \left(x_{lr} + x_m\right)/r_r$. In addition we need to implement dynamic coordinate transformation by $T(\delta_r)$ for interfacing induction motors and network algebraic equation.

Similarly, the third order model in ω_e frame can be derived as

$$\frac{p}{\omega_b}e_d = -\frac{1}{T_o'}\left[e_d + \frac{x_m^2}{\left(x_{lr} + x_m\right)}i_{qs}\right] + \left(\frac{\omega_e - \omega_r}{\omega_b}\right)e_q$$

$$\frac{p}{\omega_b}e_q = -\frac{1}{T_o'}\left[e_q - \frac{x_m^2}{\left(x_{lr} + x_m\right)}i_{ds}\right] - \left(\frac{\omega_e - \omega_r}{\omega_b}\right)e_d \tag{11}$$

The equation of motion and the definitions of the parameters are the same as (10). Eq. (9) is also valid in ω_e frame. Basically, the coordinate transformation between ω_e frame, which is rotating at the system frequency, and the frame rotating in nominal frequency should be implemented for interfacing induction motors with network algebraic equation. However, we directly connect (9) to network for simplicity. In addition, ω_e is approximated by its nominal value for simplicity.

Figure 2.3.2 shows the comparison of the two models for the motor ratio of 30%. Since the results are similar (or the same in the sense of engineering), the problem of ω_e frame model, which is raised by the authors in former subsection, is not so serious.

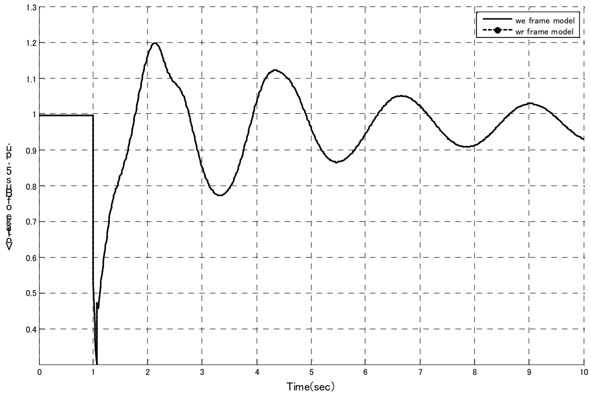

Figure 2.3.2 Comparison of ω_e and ω_r frame models (30% motor loads)

2.4 Comparison of Fifth, third and the first order models

The responses of fifth, third and first order models of induction motor have been compared. Since we assume that the fifth order model is the most accurate one, the responses of the third order model and the first order models have been compared with that of the fifth order model. The fault-duration of the system is set to 70 milli-seconds. The results show that for the lower percentage of the motor loads, the responses of all the model implementation are similar. If the percentage of the motors is increased, the lower order models give more optimistic results as compared to the response with fifth order model. Figure 2.4.1 and Figure 2.4.2 show the comparative response in 30% and 35% of the motor loads respectively. For higher percentage of the motor loads (35%), although the lower order model shows that the system is stable, the fifth order model shows that the system is unstable.

3 STABILITY COMPARISONS

3.1 Transient stability analysis

The stability limit or the maximum power transfer with the implementation of induction motor models has been evaluated in terms of loading levels. The maximum loading level (LL) is defined as the maximum percentage of bus load at which the rotor angle stability of the all the generators are maintained after the disturbance in the system. The maximum loading level was evaluated using the binary search algorithm. The motor ratio was fixed to 30% and 50% of the bus load.

The results are tabulated in the Table 1. The maximum power transfer of lower order models is larger than that of

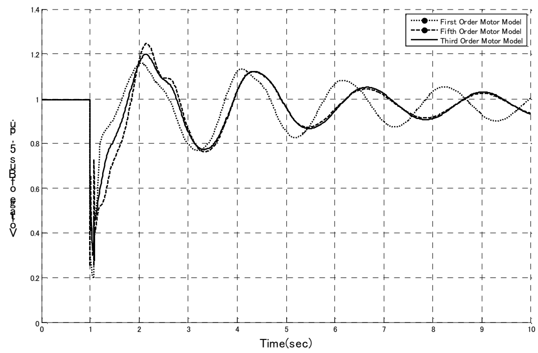

Figure 2.4.1. Comparison of responses (30% motor loads)

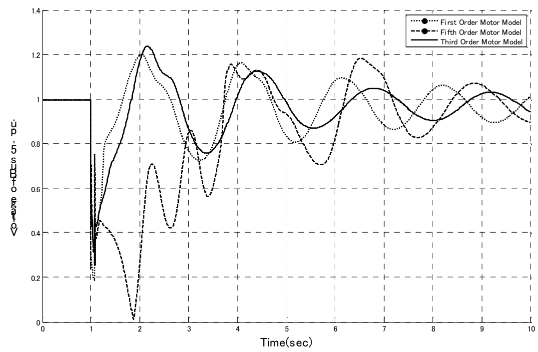

Figure 2.4.2 Comparison of responses (35% motor loads)

higher order models. This result shows the optimistic characteristics of lower order models. In addition it is shown that static load model will result in optimistic result.

The generator performance at this loading limit has also been studied. Figure 3.1.1 and Figure 3.1.2 shows the bus voltages and generator relative angle profiles at 50% of the motor loads and at the loading level of 73.4%. The result shows that the induction motor terminal voltage is near unstable due to the motor dynamics, while the generators are still in stable operation. This suggests that the voltage stability limit of the load buses is lower than the generator stability limit. Similarly, the voltage profile at the generator stability limit has been studied at loading level of 75% and motor ratio of 50% of total loads. The results are shown in Figure 3.1.3 and Figure 3.1.4. The result is very interesting because the stability of generators and induction motors are once lost and are restored finally at 6 [s] through some interaction between generators and motors.

3.2 Steady state stability analysis

The steady state stability of the system with different models of loads has been compared on the basis of eigenvalue analysis. For the load level of 100% and the induction

Table 1. Load Levels for stability limit

	Load Level	
Model	**30% Motor Load**	**50% Motor Load**
Fifth Order	1.073	0.750
Third Order	1.198	0.869
First Order	1.271	0.882
Static Loads	1.781	

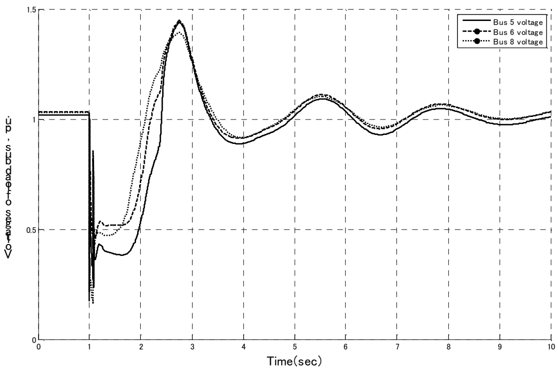

Figure 3.1.1: Voltage response at the LL= 73.4%

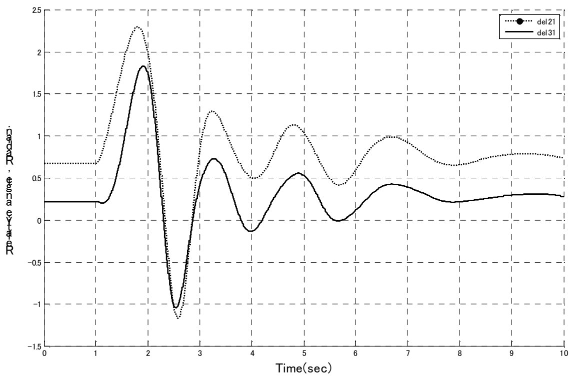

Figure 3.1.2: Generator relative angles at LL= 73.4%

motor load of 30% of the load, the eigenvalues are computed. The nature of the most significant eigenvalues that have poor damping and significant oscillatory frequency have been chosen and analyzed for the comparative study. The results are tabulated in Table 2. Also, the results for static load application are tabulated.

Note that the "slow mode" is the most significant mode because it has smaller damping coefficients than fast one. Therefore we focus on the slow mode.

When the motor loads are present, the first order model implementation gives the most optimistic stability solution. The eigenvalues of the third order model shows the stability margin similar to the fifth order model. It should be noted that the static load model results in the most conservative result. This is as opposed to the result of previous section.

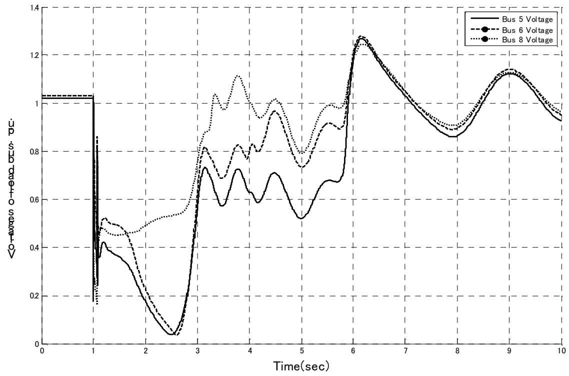

Figure 3.1.3: Load Voltages at the LL= 75%

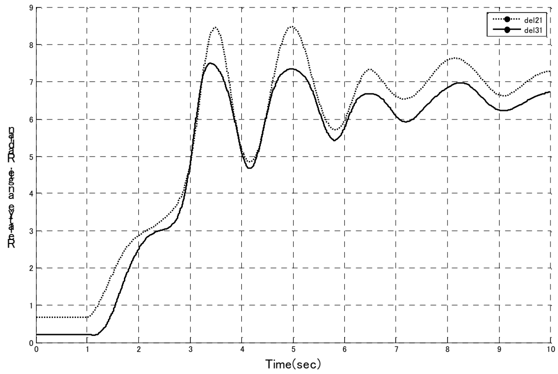

Figure 3.1.4: Generator relative angles at LL= 75%

Table 2: Comparison of eigenvalues for different models

Model	slow mode	fast mode
Fifth order	-0.199±j2.441	-0.720±j8.340
Third order	-0.191±j2.445	-0.717±j8.340
First order	-0.2195±j2.935	-0.717±j8.353
Static	-0.188±j2.937	-0.706±j8.367

4 CONCLUSIONS

In this paper, various induction motor models are compared from the viewpoint of power system stability. Induction motor models in ω_r frame, which is attached to rotor, is proposed to avoid a problem of ω_e frame models. The fifth-order, third-order and the first-order induction motor models have been developed in ω_r frame.

The transient and steady state stability of the system for the different models of the induction motor have been compared.

The results of this paper are summarized.

1. The change in system frequency results in the change in the phasor of the network quantities. The step change in phasor causes the discontinuity of the state variables in ω_e frame. The modeling of the induction motor in ω_r frame eliminates this discontinuity.

However no *practical* problem is caused by this discontinuity as a result.

2. The response of the first order, third order and the fifth order models are obviously different from each other. For the lower percentage of motor loads, the responses are similar. As the percentage of the motor increases, the responses are quite different.
3. The implementation of fifth order model gives the most conservative results of transient stability assessment and the implementation of the first order model gives the most optimistic result.
4. The application of induction motor in the load bus decreases the power transfer limit of the system. As the load level or the motor percentages are increased, the voltage instability of induction motor occurs earlier than the stepping out of the generators.
5. The eigenvalue analysis shows the higher order models represent the more poorly damped oscillations than first order model. It should be noted that static load model results in the most conservative result.

5 APPENDICES

5.1 Appendix I

First two equations in (1) can be re-written in matrix form as follows.

$$\boldsymbol{v} = \frac{1}{\omega_b}\frac{d\boldsymbol{\psi}}{dt} + \frac{1}{\omega_b}\omega_e\begin{bmatrix} 0 & 1 \\ -1 & 0 \end{bmatrix}\boldsymbol{\psi} + r\boldsymbol{i}$$

This can result in

$$\boldsymbol{v} - r\boldsymbol{i} = \frac{1}{\omega_b}\lim_{\Delta t \to 0}\frac{\left(\Delta\boldsymbol{\psi} + \Delta\delta_e\begin{bmatrix} 0 & 1 \\ -1 & 0 \end{bmatrix}\boldsymbol{\psi}\right)}{\Delta t}.$$

Since the left hand side of above equation is bounded, right hand side must be bounded. This requires

$$\left(\Delta\boldsymbol{\psi} + \Delta\delta_e\begin{bmatrix} 0 & 1 \\ -1 & 0 \end{bmatrix}\boldsymbol{\psi}\right) \to 0$$

as $\Delta t \to 0$, or

$$\Delta\boldsymbol{\psi} \to -\Delta\delta_e\begin{bmatrix} 0 & 1 \\ -1 & 0 \end{bmatrix}\boldsymbol{\psi}$$

as $\Delta t \to 0$.

On the other hand, $\Delta\delta_e$ does not approach to zero as $\Delta t \to 0$ at the moment of discontinuity of δ_e. At this time, $\Delta\boldsymbol{\psi} \neq 0$ from above relationship and then discontinuity of $\boldsymbol{\psi}$ is implied.

5.2 Appendix II

Power system under study:

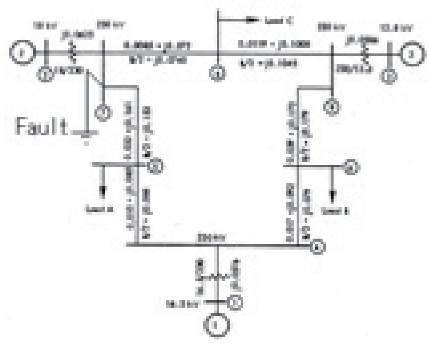

6 REFERENCES

[1]. C. Concordia and S. Ihara, "Load representation in power system stability studies," *IEEE Trans. Power App. Syst., vol. PAS-101, pp. 969-977, 1982.*

[2]. D. N. Kosterev, C. W. Taylor, and W. A. Mittelstadt, "Model validation for the August 10, 1996 WSCC system outage," *IEEE Trans. Power Syst., vol. 14, pp. 967-979, Aug. 1999.*

[3]. L. Pereira, D. Kosterev, P. Mackin, D. Davies, J. Undrill, W. Zhu," An interim dynamic induction motor model for stability studies in the WSCC", *IEEE Trans.Power Syst., vol. 17, Nov. 2002.*

[4]. M. Jin, H. Renmu and David J. Hill," Load modeling by finding support vectors of load data from field measurements", IEEE Trans. Power Systems, VOL 21,No. 2, May 2006.

[5]. H. Renmu, M. Jin, David J. Hill," Composite load modeling via measurement approach", *IEEE Trans. Power Systems, VOL 21,No. 2, May 2006.*

[6]. B.K. Choi, H.D. Chiang, Y. Li, H. Li, Y.T. Chen, D.H. Huang, and M.G. lauby," Measurement based dynamic load models: derivation, comparison and validation", *IEEE Trans. Power Systems, VOL 21,No. 3, August 2006.*

[7]. B.C. Lesieutre, P.W. Sauer, M.A. Pai, " Development and comparative study of induction machine based dynamic P,Q load models", *IEEE Transactions on Power Systems, Vol. 10, No. 1, February 1995*

[8]. Y. Kataoka, T. Omata, " On input/output variables of load model for stability studies", *IEEJ Trans. Power and energy, no. 1347, 1999*

[9]. X. Xu, R.M. Mathur, J.Jiang, G.J. Rogers, P. Kundur, "Modeling effects of system frequency variations in induction motor dynamics using singular perturbations", *IEEE Transactions on Power Systems, Vol.15, No 2, May 2000*

[10]. A. Borghetti, R. Caldon, A. Mari, C.A. Nucci, "On dynamic load models for voltage stability studies", *IEEE Transactions on Power Systems, Vol. 12, No. 1, February 1997.*

[11]. P.C. Krause, C.H. Thomas, "Simulation of Symmetrical Induction Machinery", *IEEE transactions on power apparatus and systems, Vol. PAS-84, No. 11. November 1965*

[12]. P. Kundur, "Power system stability and control", *Electric Power Research Institute*